THE JOURNAL OF THE ACOUSTICAL SOCIETY OF KOREA Vol.22, No.1E 2003. 3. pp. 11~18

Exterior Acoustic Holography Reconstruction of a Tuning Fork Using Inverse Non-singular BEM

Soon-Suck Jarng*
*Dept. of Information Control & Instrumentation, Chosun University, Korea
(Received September 13 2003; accepted February 18 2003)

Abstract

Non-singular boundary element method (BEM) codes are developed in acoustics application. The BEM code is then used to calculate unknown boundary surface normal displacements and surface pressures from known exterior near field pressures. And then the calculated surface normal displacements and surface pressures are again applied to the BEM in forward in order to calculate reconstructed field pressures. The initial exterior near field pressures are very well agreed with the later reconstructed field pressures. Only the same number of boundary surface nodes (1178) are used for the initial exterior pressures which are at first calculated by Finite Element Method (FEM) and BEM. Pseudo-inverse technique is used for the calculation of the unknown boundary surface normal displacements. The structural object is a tuning fork with 128.4 Hz resonant. The boundary element is a quadratic hexahedral element (eight nodes per element).

Keywords: *BEM, Holography, Tuning fork, 3 Dimensions, Non-singular, Inverse BEM, Pressure field*

I. Introduction

Electro-mechanical devices such as motor and engine generate sound with noise. Unless the noise-like sound is non-stationary, it is possibly easier to find where is the origin of the noise sound. The stationary noise source may be pointed out by an acoustic holographic technique in which an array of microphones measure the sound pressure field in three dimensions surrounding an interesting noise radiating object in order to geometrically analyze the position of the noise source. The acoustic holographic technique may be approached by either Spatial Fourier Transformation (SFT)[1,2] or Inverse Boundary Element Method (BEM)[3,4]. In both approaches, spatial sound pressures of a single frequency are measured known complex values and the target of the acoustic holography is to calculate either the unknown surface pressure or the normal velocity of the specimen. Then the near or far filed sound pressure may be recalculated, so as to reconstruct the original 3 dimensional sound pressure field. This paper presents an inverse non-singular BEM technique for the acoustic holographic analysis. The sound radiating object is a tuning fork. The analysis is done in 3 dimensions. In order to simulate the acoustic holography with the neglect of the measurement signal noise of the spatial sound pressure, the forward BEM supplied the three dimensional sound field pressures as the initially known complex values.

Corresponding author: Soon-Suck Jarng (ssjarng@mail.chosun.ac.kr)
Dept. of Information Control & Instrumentation, Chosun Uni.
375 SeoSeok-Dong, Dong-Ku, Gwang-Ju 501-759, Korea

II. Numerical Methods

2.1. Finite Element Method (FEM)

The following equation (1) is the integral formulation

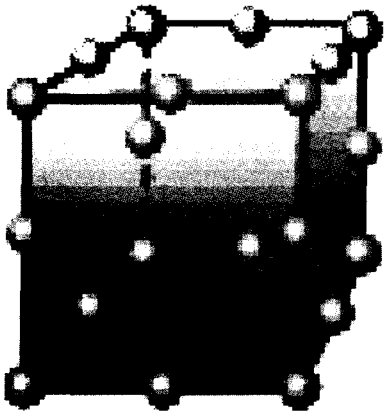

Figure 1. Three dimensional quadratic hexahedral 20 nodes element.

of the FEM elastic equations:

$$\{F\}=[K]\{a\}-\omega^2[M]\{a\} \tag{1}$$

The isoparametric formulation for 3-dimensional structural elements is well documented by Allik H. et. al.[5]. Each 3-dimensional finite element is composed of 20 quadratic nodes and each node has nodal displacement (a_x, a_y, a_z) variables. In local coordinates the finite element has 6 surface planes ($\pm$xy, $\pm$yz, $\pm$zx) which may be exposed to external air environment. The exposed surface is used as a boundary element which is composed of 8 quadratic nodes.

2.2. Boundary Element Method (BEM)

The boundary element solution of sound pressure intensity is very useful to analyze the sound radiation of vibrating devices; intensity, directivity pattern and noise control elements. For sinusoidal steady-state problems, the Helmholtz equation, $\nabla^2\Psi+k^2\Psi=0$ represents the fluid mechanics. Ψ is the acoustic pressure with time variation, $e^{j\omega t}$. In order to solve the Helmholtz equation in an infinite air media, a solution to the equation must not only satisfy structural surface boundary condition (BC), $\partial\Psi/\partial n=\rho_f\omega^2 a_n$ but also the radiation condition at infinity, $\lim_{|r|\to\infty}\oint s(\partial\Psi/\partial r+jk\Psi)^2dS=0$. $\partial/\partial n$. represents differentiation along the outward normal to the boundary.

The Helmholtz integral equation derived from Green's second theorem provides such a solution for radiating pressure waves;

$$\int_S\left(\Psi(q)\frac{\partial G_k(p,q)}{\partial n_q}-G_k(p,q)\frac{\partial\Psi(q)}{\partial n_q}\right)dS_q=\beta(p)\,\Psi(p) \tag{2}$$

where $G_k(p,q)=e^{-jkr}/4\pi r$, $r=|p-q|$

p is any point in either the interior or the exterior and q is the surface point of integration. β (p) is the exterior solid angle at p.

The acoustic pressure for the i^{th} global node, $\Psi(p_i)$, is expressed in discrete form[6]: $(1\le i\le ng)$

$$\beta(p_i)\Psi(p_i)=\int_S\left(\Psi(q)\frac{\partial G_k(p_i,q)}{\partial n_q}-G_k(p_i,q)\frac{\partial\Psi(q)}{\partial n_q}\right)dS_q \tag{3a}$$

$$=\sum_{m=1}^{nt}\int_{S_m}\left(\Psi(q)\frac{\partial G(p_i,q)}{\partial n_q}-G(p_i,q)\frac{\partial\Psi(q)}{\partial n_q}\right)dS_q \quad q\in S_m \tag{3b}$$

$$=\sum_{m=1}^{nt}\int_{S_m}\left(\sum_{j=1}^{8}N_j(q)\Psi_{m,j}\frac{\partial G(p_i,q)}{\partial n_q}-G(p_i,q)\sum_{j=1}^{8}N_j(q)\frac{\partial\Psi_{m,j}}{\partial n_q}\right)dS_q \tag{3c}$$

$$=\sum_{m=1}^{nt}\sum_{j=1}^{8}\left(\int_{S_m}N_j(q)\frac{\partial G(p_i,q)}{\partial n_q}dS_q\right)\Psi_{m,j}-\rho_f\omega^2\sum_{m=1}^{nt}\sum_{j=1}^{8}\left(\int_{S_m}N_j(q)G(p_i,q)n_q dS_q\right)a_{m,j} \tag{3d}$$

$$=\sum_{m=1}^{nt}\sum_{j=1}^{8}A^i{}_{m,j}\Psi_{m,j}-\rho_f\omega^2\sum_{m=1}^{nt}\sum_{j=1}^{8}B^j{}_{m,j}a_{m,j} \tag{3e}$$

where nt is the total number of surface elements and $a_{m,j}$ are three dimensional displacements.

Equation (3b) is derived from equation (3a) by discretizing integral surface. And equation (3c) is derived from equation (3b) since an acoustic pressure on an integral surface is interpolated from adjacent 8 quadratic nodal acoustic pressures corresponding the integral surface. Then equation (3d) is derived from equation (3c) by swapping integral notations with summing notations. Finally the parentheses of equation (3d) is expressed by upper capital notations for simplicity.

When equation (3e) is globally assembled, the discrete Helmholtz equation can be represented as

$$[A]-\beta[I]\{\Psi\}=+\rho_f\omega^2[B]\{a\} \tag{4}$$

where [A] and [B] are square matrices of (ng by ng) size.

ng is the total number of surface nodes.

When the impedance matrices of equation (4), [A] and [B], are computed, two types of singularity arise[7]. One is that the Green's function of the equation, $G_k(p_i, q)$, becomes infinite as q approaches to p_i. This problem is solved by mapping such rectangular local coordinates into triangular local coordinates and again into polar local coordinates[8]. The other is that at certain wave number the matrices become ill-conditioned. These wave number are corresponding to eigenvalues of the interior Dirichlet problem[9]. One approach to overcome the matrix singularity is that [A] and [B] of equation (4) are modified to provide a unique solution for the entire frequency range [10-13]. The modified matrix equation referred to as the modified Helmholtz gradient formulation (HGF)[13] is obtained by adding a multiple of an extra integral equation to equation (4).

$$([A]-\beta[I]\oplus\alpha[C])\{\Psi\}=+\rho_f\omega^2([B]\oplus\alpha[D])\{a\} \tag{5}$$

where $\alpha=\frac{\sqrt{-1}}{k\cdot(\text{Number of surface element adjacent a surface node})}$

[C] and [D] are rectangular matrices of (nt by ng) size. $\ominus$ symbol indicates that the rows of [C], [D] corresponding to surface elements adjacent a surface node are added to the row of [A], [B] corresponding to the surface node, that is,

$$\begin{aligned}\sum_{i=1}^{ng}\sum_{j=1}^{ng}A(i,j)&=\sum_{i=1}^{ng}\sum_{j=1}^{ng}A(i,j)+\sum_{i=1}^{ng}\sum_{j=1}^{ng}\left(\sum_{m=1}^{s(i)}\alpha\ C(m,j)\right)\\ \sum_{i=1}^{ng}\sum_{j=1}^{ng}B(i,j)&=\sum_{i=1}^{ng}\sum_{j=1}^{ng}B(i,j)+\sum_{i=1}^{ng}\sum_{j=1}^{ng}\left(\sum_{m=1}^{s(i)}\alpha\ D(m,j)\right)\end{aligned} \tag{6}$$

where S(i) is the number of surface element adjacent a surface node. The derivation of the extra matrices [C], [D] are well described by Francis D.T.I.[13]. Equation (6) may be reduced in its formulation using superscript $\oplus$ for convenience;

$$A^{\oplus}\{\Psi\}=+\rho_f\omega^2B^{\oplus}\{a\} \tag{7}$$

where $([A]-\beta[I]\oplus\alpha[C])=A^{\oplus}$, $([B]\oplus\alpha[D])=B^{\oplus}$

Equation (7) can be written as

$$\{\Psi\}=+\rho_f\omega^2\left(A^{\oplus}\right)^{-1}B^{\oplus}\{a\} \tag{8}$$

Since the present acoustic vibrator produces displacement data $\{a\}$ at a natural frequency, the surface pressure $\{\Psi\}$ of the tuning fork is calculated from equation (8). Once $\{a\}$ and $\{\Psi\}$ are known, the acoustic pressure in the far field is determined by $\beta(p)=1$ of equation (2) for given values of surface nodal pressure and surface nodal displacement;

$$\Psi(p_i)=\sum_{m=1}^{nt}\sum_{j=1}^{8}A^i{}_{m,j}\Psi_{m,j}-\rho_f\omega^2\sum_{m=1}^{nt}\sum_{j=1}^{8}B^i{}_{m,j}\,a_{m,j} \tag{9}$$

2.3. Pseudo Inverse BEM

Previously mentioned forward BEM solves unknown near/far field acoustic pressures once the surface displacement vector and the surface pressure scalar of the vibrating tuning fork are known. Equation (8) calculates the surface pressures from the given 3 dimensional surface displacement vectors which are supplied by the FEM equation (1). Therefore the finally calculated near field acoustic pressures derived by equation (9) may be indirectly used as if initially measured sound pressures for the acoustic holographic approach. These calculated near field acoustic pressures are notified as an original (initial) input sound pressures. The number of the original input sound pressures are taken as the same as the number of unknown surface pressures, that is, the number of the surface nodes (ng).

Now the next step is to inversely find the unknown surface pressure or surface displacement from the known near filed sound pressure. Equation (3) as well as the following equations (3~9) are modified, so that the displacement vector is changed to the normal displacement scalar. It ensures that $A^{\oplus}$ and $B^{\oplus}$ have the same matrix sizes as ng by ng.

$$\{\Psi\}=+\rho_f\omega^2\left(A^{\oplus}\right)^{-1}B^{\oplus}\{a_n\} \tag{10}$$

Equation (9) can be reformulated as

$$A_1\{\Psi\}+B_1\{a_n\}=\{\Psi_f\} \tag{11}$$

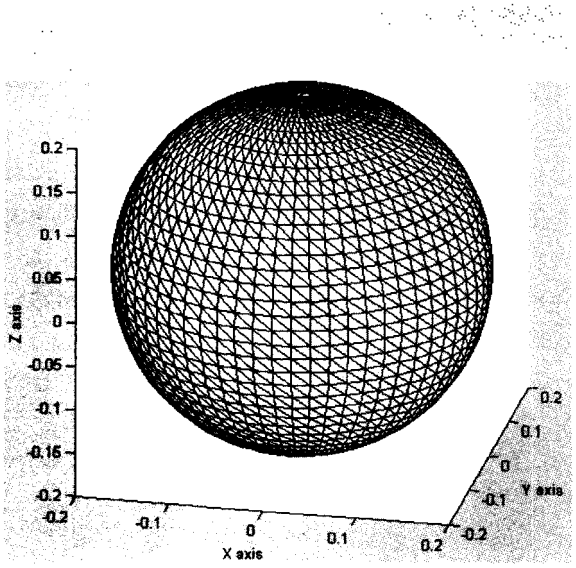

Figure 2. Three dimensional near field original sound pressure positions.

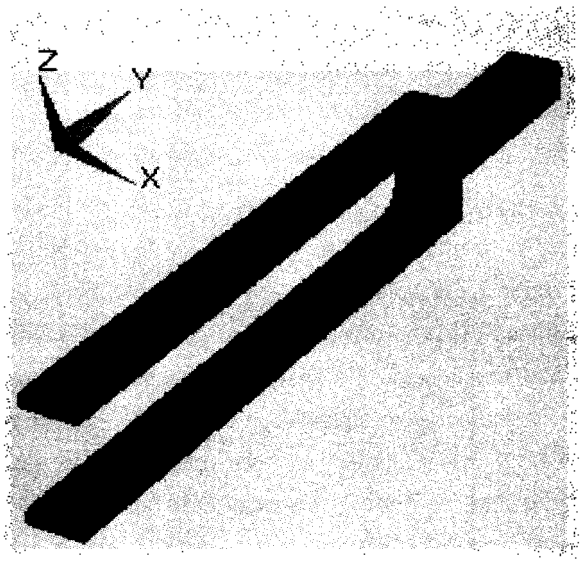

Figure 3. Three dimensional tuning fork FEM elements. Length =152.4 [mm], Width=25.4 [mm], Material=Steel (4130).

And if equation (10) is added into equation (11),

$$\left(\rho_f \omega^2 A_1 \left(A^{\oplus}\right)^{-1} B^{\oplus} + B_1\right)\{q_n\} - G\{q_n\} = \{\Psi_f\} \tag{12}$$

Equation (12) is solved by pseudo inverse matrix technique which is derived by singular value decomposition (SVD) since the coefficient matrices of equation (12) have complex values. If the SVD of G matrix is $U\Lambda W^H$, then

$$\{q_n\} = W\Lambda^{-1}U^H\{\Psi_f\} \tag{13}$$

The size of G matrix is ng by ng. If more than ng near filed sound pressures are supplied, then the number of rows in G matrix is more than the number of columns in G matrix. Even though G becomes rectangular matrix, equation (13) can be still solved because the SVD provide singular values from the highest order.

III. Results

3.1. Tuning Fork FEM Application

The FEM is applied to the analysis of the tuning fork. Figure 3 shows 3 dimensional tuning fork FEM elements and Table 1 shows the material properties of the air and the steel.

Table 1. Material Properties.

	Density (ρ) [Kg/m^3]	Young's Modulus (E) [N/m^2]	Poisson Ratio (ν)
Air	1.22	1.411E5	-
Steel	7822.9	2.0684E11	0.30

The tuning fork has the first modal frequency at 128.4 Hz. Figure 5 shows the 3 dimensional modal shape at the first mode.

3.2. Tuning Fork Forward BEM Application

The surface pressure of the tuning fork is calculated by equation (8) from the given surface displacement provided by the FEM eigenvectors. Then the so-called original near field acoustic pressures in 3 dimensions are calculated by equation (9) at the same first modal frequency, 128.4 Hz. Figure 6 shows the directivity pattern of the tuning fork in 2 dimensions' view. And Figure 7 shows the directivity pattern of the tuning fork in 3 dimensions.

3.3. Tuning Fork Pseudo Inverse BEM Application

Only normal surface displacements are considered in the pseudo inverse BEM. The normal surface displacement of the tuning fork is calculated by equation (13) from the

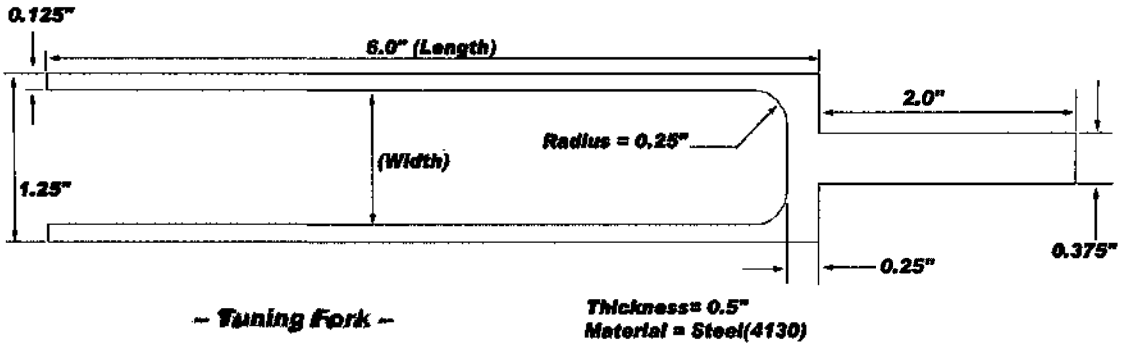

Figure 4. Tuning fork dimensions.

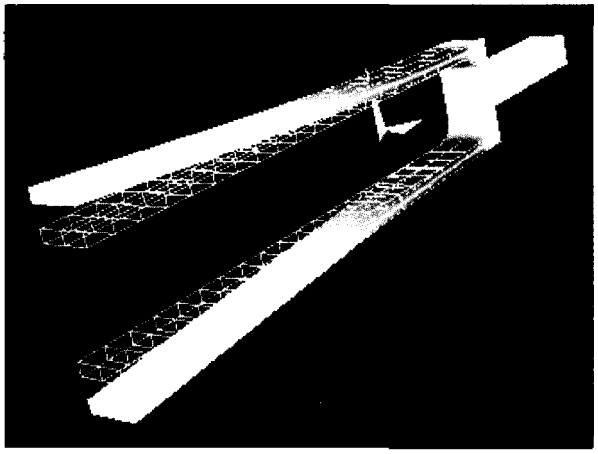

Figure 5. Modal shape of tuning fork (Color=Von Mises Stress) at 128.4 Hz (1st mode).

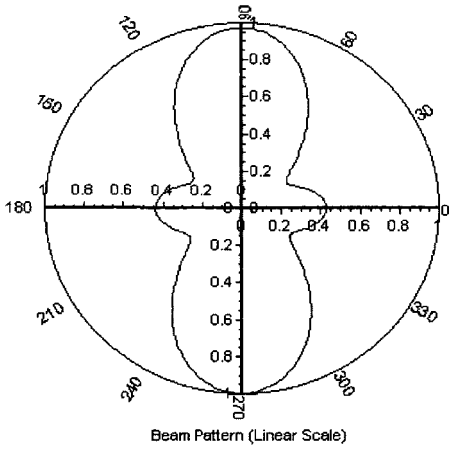

Figure 6. Beam pattern of tuning fork in 2 dimensions.

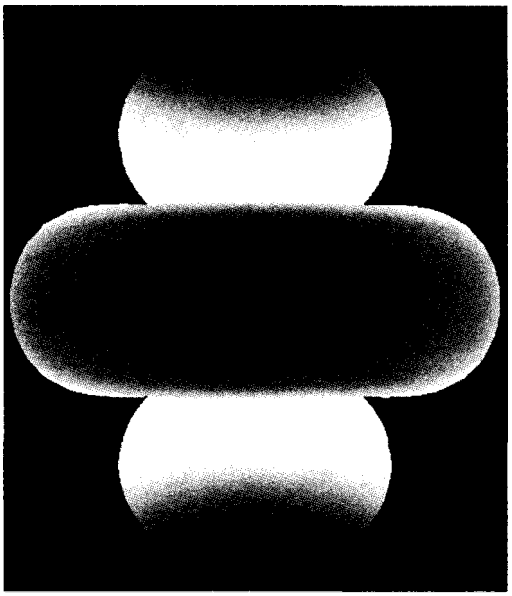

Figure 7. Beam pattern of tuning fork in 3 dimensions.

supplied exterior near field acoustic pressures which are complex values. Then The surface pressure of the tuning fork is calculated by equation (10). Figure 8 (a) and (b) show the real and the imaginary surface pressures of the tuning fork respectively. The blue continuous lines indicate the original surface pressure of the tuning fork derived by equation (8) while the red dotted lines indicate the recalculated surface pressure of the tuning fork derived by equation (10).

And figure 9 shows the 3 dimensional deformed shape of the tuning fork drawn from the recalculated normal surface displacement. It should be noted that the overall deformed shape of the tuning fork is quite similar to that of the originally displaced tuning fork, that is, the two ends of the bars are significantly deformed in +Z and -Z axes directions. The main difference between figure 9 and figure 5 is that the inner surfaces of the tuning fork ends

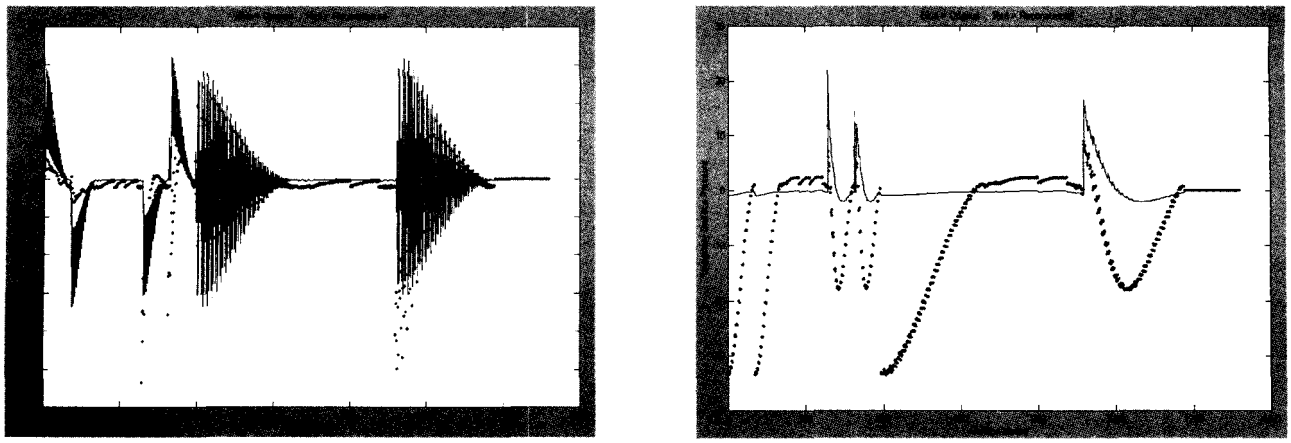

(a) (b)

Figure 8. The real (a) and the imaginary (b) surface pressures of the tuning fork. The blue continuous lines = Original surface pressure, The red dotted lines = Recalculated surface pressure.

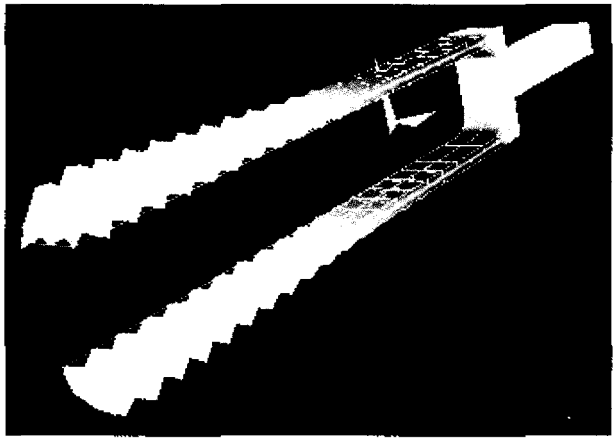

Figure 9. Three dimensional deformed shape of the tuning fork drawn from the recalculated normal surface displacement (Color=Von Mises Stress).

have much smaller displacements than the outer surfaces of the tuning fork ends.

Figure 10 (a) and (b) show the real and the imaginary near field sound pressures of the tuning fork respectively. The blue continuous lines indicate the original near field pressure of the tuning fork while the red dotted lines indicate the reconstructed near field pressure of the tuning fork. Both original and reconstructed near field pressures are almost perfectly agreed each other.

Figure 11 shows the reconstructed directivity pattern of the tuning fork in 3 dimensions.

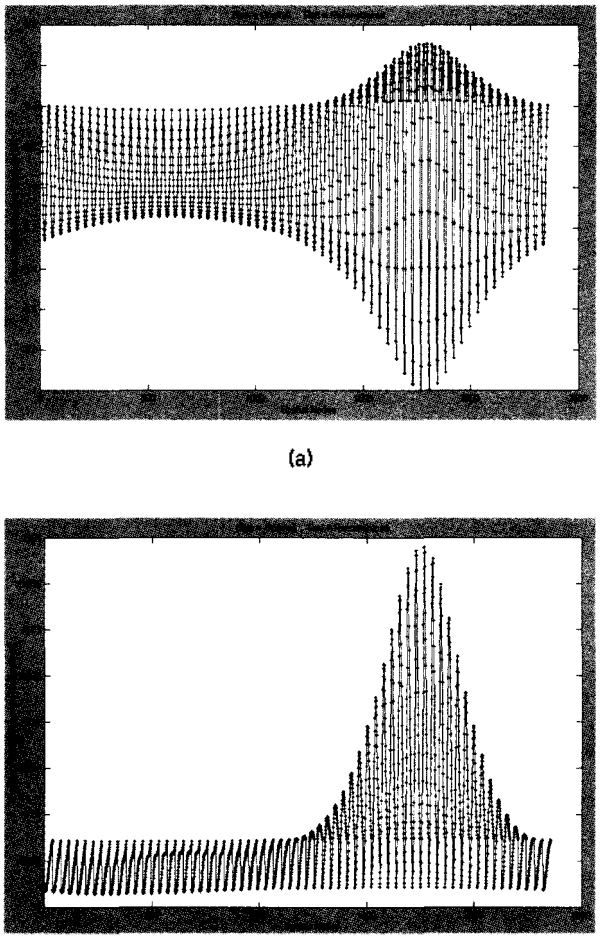

(a)

(b)

Figure 10. The real (a) and the imaginary (b) near field acoustic pressures of the tuning fork. The blue continuous lines = Original near field pressure, The red dotted lines = Reconstructed near field pressure.

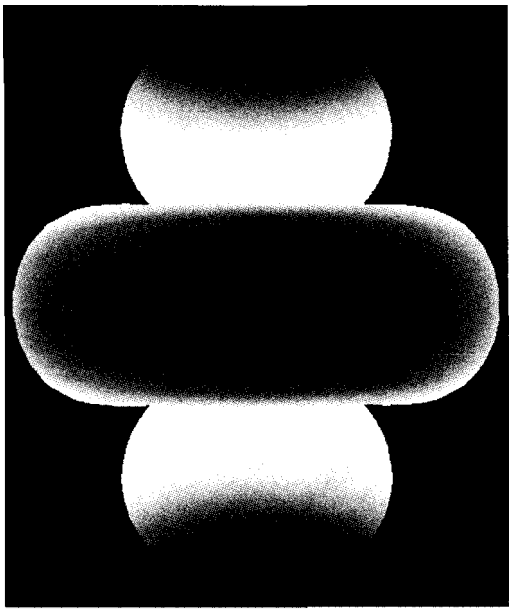

Figure 11. Reconstructed beam pattern of tuning fork in 3 dimensions.

IV. Conclusion

Non-singular BEM codes are developed in acoustics application. The BEM code is then used to calculate unknown boundary surface normal displacements and surface pressures from known exterior near field pressures. And then the calculated surface normal displacements and surface pressures are again applied to the BEM in forward in order to calculate reconstructed field pressures. The initial exterior near field pressures are very well agreed with the later reconstructed field pressures. The next study would be adding noise effects to the original sound field pressures and adding more number of exterior sound field pressures to overcome noise-induced measurements.

Symbol Notification

$\{F\}$	Applied Mechanical Force
$\{a\}$	Elastic Displacement
$[K]$	Elastic Stiffness Matrix
$[M]$	Mass Matrix
ω	Angular Frequency
ρ_f	Fluid (Air) Density
a_n	Normal Displacement on the Structural Surface
k	Wave Number ($= \omega/c$)
c	Sound Speed in Air; 340 [m/sec]
ng	Number of Surface Nodes
nt	Number of Surface Elements
$\{a\}$	Displacement Vector on the Structural Surface
$\{\Psi\}$	Pressure Vector on the Structural Surface
$\{\Psi_f\}$	Near Field Pressure Vector

Acknowledgments

This study was supported by research fund from Chosun University, 2002.

References

1. J. D. Maynard, E. G. Williams and Y. Lee, "Nearfield acoustic holography; I. Theory of generalized holography and the development of NAH," *J. Acoust. Soc. Am.*, **78** (4), 1395-1413, 1985.
2. W. A. Veronesi and J. D. Maynard, "Nearfield acoustic holography; II. Holographic reconstruction algorithms and computer implementation," *J. Acoust. Soc. Am.*, **81** (5), 1307-1322, 1987.
3. W. A. Veronesi and J. D. Maynard, "Digital holographic reconstruction of source with arbitrary shaped surfaces," *J. Acoust. Soc. Am.*, **85** (2), 588-598, 1989.
4. K. Gardner and R. J. Bernhard, "A noise source identification technique using an inverse Helmholtz integral equation method," *Trans. ASME, J. Vib. Acoust. Stress Reliab. Des.*, **110**, 84-90, 1988.
5. H. Allik and T. J. R. Hughes, "Finite element method for piezoelectric vibration," *Int. J. Numer. Method Eng.*, 2, 151-157, 1970.
6. L. G. Copley, "Integral equation method for radiation from vibrating bodies," *J. Acoust. Soc. Am.*, **41**, 807-816, 1967.
7. L. G. Copley, "Fundamental results concerning integral representations in acoustic radiation," *J. Acoust. Soc. Am.*, **44**, 28-32, 1968.
8. E. Skudrzyk, "The foundation of acoustics," Springer-Verlag, New York, Equation (76), 408-409, 1971.
9. D. T. I. Francis, "A boundary element method for the analysis of the acoustic field in three dimensional fluid-structure interaction problems," *Proc. Inst. of Acoust.*, 12, Part 4, 76-84, 1990.
10. H. A. Schenck, "Improved integral formulation for acoustic radiation problems," *J. Acoust. Soc. Am.*, **44**, 41-58, 1968.
11. A. J. Burton and G. F. Miller, "The application of integral

integration methods to the numerical solutions of some exterior boundary problems," *Proc. R. Soc. London, Ser.*, A 323, 201-210, 1971.
12. R. F. Kleinman and G. F. Roach, "Boundary integral equations for the three dimensional Helmholtz equation," *SIAM Rev.*, **16**, 214-236, 1974.
13. D. T. I. Francis, "A gradient formulation of the Helmholtz integral equation for acoustic radiation and scattering," *J. Acoust. Soc. Am.*, **93** (4) Part 1, 1700-1709, 1993.

[Profile]

• Soon-Suck Jarng

1984. 2: Hanyang Uni. (S. Korea), Dept. of Electronics (B.Eng.)
1985. 9: Hull Uni. (U.K.), Dept. of Electronics (M.Eng.)
1988. 9: Birmingham Uni. (U.K.), Dept. of Physiology (M.Sc.)
1991. 12: Birmingham Uni. (U.K.), Dept. of Electronic Electrical Eng. (Ph.D.)
1992. 3~Present: Chosun Uni. (S. Korea), Dept. of Information Control & Instrumentation

※ Main Research: Cochlear Bio-mechanics, Underwater/Underground Acoustics, Piezoelectric Sensor Device,
Finite Element Method (FEM), Boundary Element Method (BEM)